KONINKLIJK NEDERLANDS METEOROLOGISCH INSTITUUT

WETENSCHAPPELIJK RAPPORT

SCIENTIFIC REPORT

W.R. 83 - 15

H.R.A. Wessels

Distortion of the wind field by the Cabauw meteorological tower

De Bilt, 1983

Publikatienummer: K.N.M.I. W.R. 83-15 (FM)

Koninklijk Nederlands Meteorologisch Instituut,
Fysisch Meteorologisch Onderzoek,
Postbus 201,
3730 AE De Bilt,
Nederland.

U.D.C.: 551.501.75 :
551.507.7

Distortion of the wind field by the Cabauw meteorological tower

H.R.A. Wessels

Abstract

Measurements of wind direction and velocity at and near the Cabauw meteorological tower are disturbed by the tower, a measuring building and various supporting constructions. Potential flow theory has been used to describe the flow around these obstacles and along their downwind wakes. The presence of a wake contributes significantly to the size of the measuring errors. Correction formulae are presented for the Cabauw data set of the years 1973-1984. These results have been validated by comparing simultaneous measurements at different instrument positions.

Contents

1. Introduction

Since December 1972 wind velocity and wind direction have been measured along the 213 m meteorological tower of Cabauw. The wind measurements at the 20 m level and higher take place at a distance of about 10 radii from the axis of the cylinder-shaped tower. In the planning stage this distance was assumed sufficient to restrict upstream velocity errors to less than 1% (Van Ulden et al., 1976). This estimate was based on published results considering laminar potential flow around cylindrical masts. However, in 1973 already, larger differences between simultaneous measurements at different booms were detected. These were ascribed to flow disturbances caused by the booms and the side arms (van der Vliet, 1981). Therefore it was decided to apply 0.5 m extension tubes under the cups and vanes. The present report proceeds with the comparisons made after the introduction of these extension tubes in early 1977.

It can be demonstrated - both theoretically and experimentally - that flow disturbances by mast and boom cause errors up to 4 percent in velocity and 3 deg in direction. Even larger errors occur at one of the auxiliary masts. The difference with earlier estimates is caused by the inclusion of the obstacle's wake in the potential flow calculations. Then the errors decline no longer with the square distance from the obstacle but with the distance itself.

As a result of this study correction formulae are suggested that almost completely remove these important systematic errors.

2. Brief description of the measurement positions

The instrument positions in the subsequent years are summarized in Table 1. Apart from the redistribution of instruments between the periods considered the major changes were the insertion of extension tubes in 1977 and the use of propeller vanes after 1981.

The mast and its surroundings have been described elsewhere (van Ulden et al., 1976, van der Vliet, 1981). The most important instrument positions are illustrated in Figures 1 and 2.

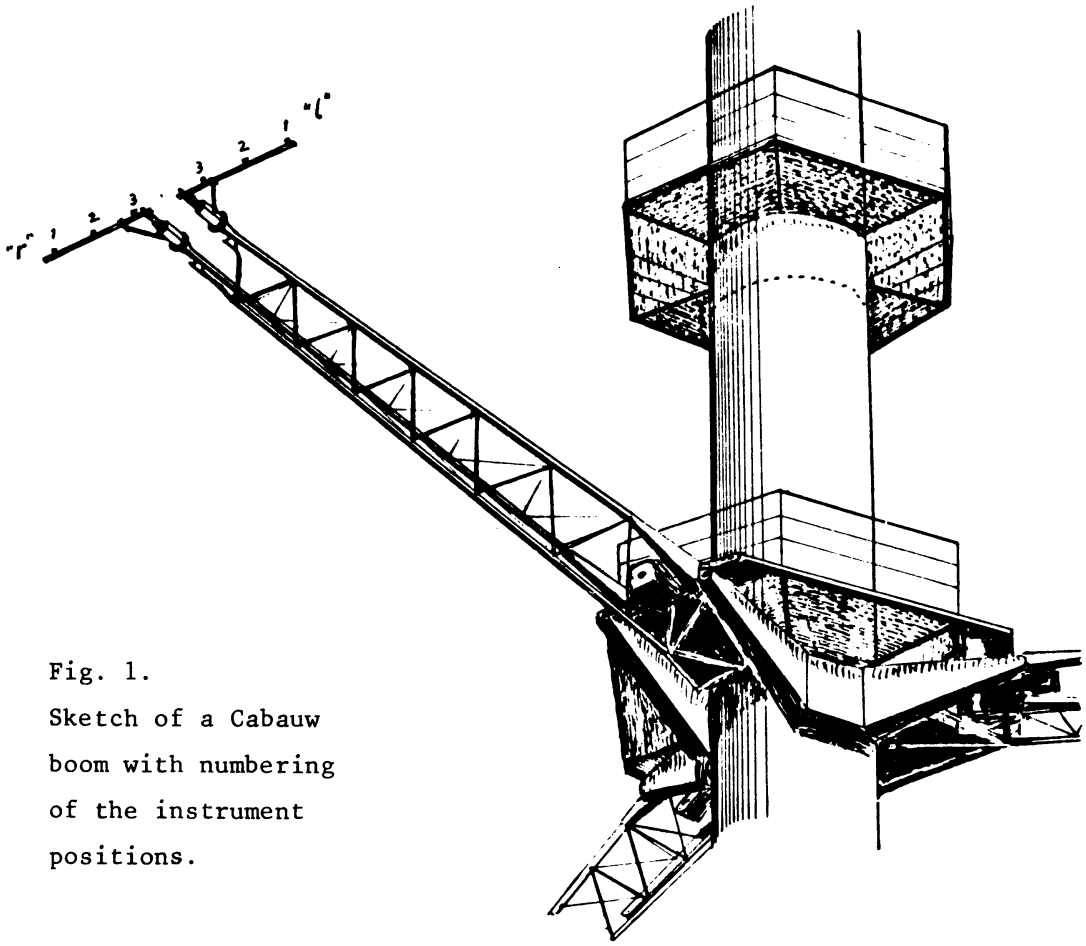

Fig. 1.
Sketch of a Cabauw boom with numbering of the instrument positions.

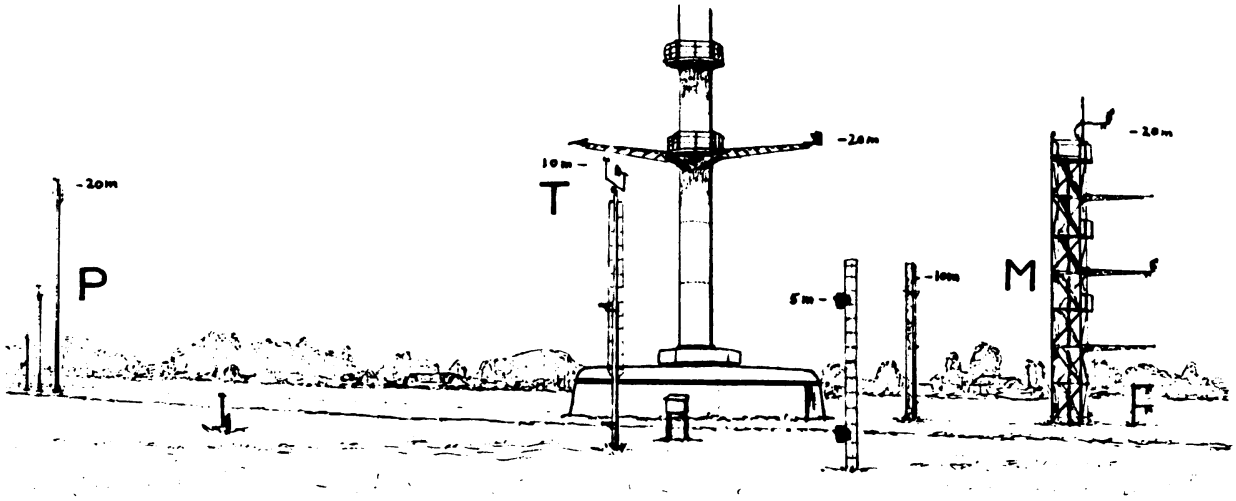

Fig. 2. View of the Cabauw main tower and auxiliary masts as seen from the south.

Table 1. Position of routine wind-measuring equipment at Cabauw. Indicated are the three boom-directions, the separate masts to the NW(P), SE(M) and S(T), the left and right (l/r) side-extensions of the booms and the plug positions numbered 1, 2, 3 from the outside, resp. at 1.35, 0.80 and 0.45 m from the boom axis (see also Fig. 1).

Year:	1973-1976	1977-1979 with (changes → 77/78)	1981-1984 (vanes at SE only)
Direction			
200 m	Nr_3 SEr_3 SWr_3	Nl_2 SEr_2 SWr_2	Nr_1 (SE) SWl_1
160 m		Nl_2 SEr_2 SWr_2	Nr_1 SWl_1
120 m	Nr_3 SEr_3 SWr_3	Nl_2 SEr_2 SWr_2	Nr_1 SWl_1
80 m		Nl_2 SEr_2 SWr_2	Nr_1 (SE) SWl_1
20 m		Nl_2 SEr_2 SWr_2	Nr_1 (SE) SWl_1
(M=15m) 20 m		Nl_2 M SWr_2	P (M) SWl_1
10 m	T		
Velocity			
200 m	Nr_1 SEr_1 SWr_1	Nr_1 SWl_1	Nr_1 SWl_1
160 m		Nr_1 SWl_1	Nr_1 SWl_1
120 m		Nr_1 SWl_1	Nr_1 SWl_1
80 m	Nr_1 SEr_1 SWr_1	Nr_1 SWl_1	Nr_1 SWl_1
40 m		Nr_1 SWl_1	Nr_1 SWl_1
20 m		$Nr_1 \rightarrow P$ M SWl_1	P M
10 m	T	$T \rightarrow P$ M	P M
5 m		P M	
1.5 m		$T \rightarrow P$ M	

Flow disturbance of the measurements along the main tower can be expected from:

- the main tower itself, being a cylinder of 2 m diameter,
- the balconies although these are an open-lattice construction,
- the booms,
- their side-arms,
- the instruments and their housings.

At every measuring level three booms are available, allowing the measurements to be made at 10.4 m from the tower axis. The boom directions are approximately 12 deg ± 120 deg at 200 m, 9 deg ± 120 deg at 20 and 160 m and 8 deg ± 120 deg at the 40 m, 80 m and 120 m levels. The booms consist of an open construction with three tubular 0.07 m diameter beams. They end at two connection boxes (0.24 x 0.12 x 0.12 m^3) which carry the side extensions of 0.06 m tubing. (Details are shown in Fig. 1).

Measurements below 40 m are not only disturbed by the tower but also by the 3.75 m high, 17 m diameter building at its foot. The actual disturbance depends on the location of the auxiliary mast (Fig. 2):

- P-masts, all at 305 deg azimuth. A 20 m high mast at 73 m distance with a separate 10 m mast at 79 m and a 5 m mast at 86 m.
- M-mast, at 130 deg and 29 m with small booms at the 5,10 and 15 m levels extending to 34 m from the main tower axis.
- T-mast at 180 deg and 72 m distance.

Next we consider the possible contribution of supporting constructions to the disturbance of these low level measurements.

- P-masts. Two anemometers (later propellervanes) were in an almost ideal position at the top of separate masts.
  The anemometers at 5 m and 1.5 m height were at 1 m distance (azimuth 305 deg) from a 0.07 m diameter vertical supporting tube.
- M-mast. This consists of a lattice-type construction with rectangular cross-section 2 x 1.6 m^2 (short side facing the instruments). The mast has seven sections with balconies and corresponding flights of stairs (fig. 2). Although the construction is rather open we might expect some flow effects. The booms themselves are shortened versions of the main mast booms. They compare favourably regarding the flow disturbance because the booms and the side-arms are missing here. The 1.5 m wind is measured exactly under the 5 m instrument position and has a 0.07 m cylinder at 1 m distance (310 deg). The wind speed at 20 m is measured on a horizontal tube extending 1.7 m (130 deg) from and 1 m above the top balcony handrail.

- T-mast. The anemometer plug was 0.73 m to the SW of the vane plug, but the latter was 0.65 m lower. The wind speed is therefore hardly disturbed but the wind direction might be influenced during north-easterly winds.

The exact position where the meteorological quantity is measured depends on the type of sensor. See table 2.

Table 2. Measuring location for various instruments. The figures for extension tubes are within brackets.

(m)	vertical distance from axis side-arm (0.10 m plug)	horizontal distance measured upwind from plug
anemometer	0.24 (0.74)	0
wind vane	0.32 (0.82)	0.29
prop. vane	0.63	0.23/+0.43
trivane	0.67 (0.80 later)	-0.14/+0.26

3. Survey of instrumental wind direction errors

Wind direction measurements deserve special attention because they proved less reliable than the velocity measurements. As an example of the quality of the latter we may mention that cup anemometer and propeller calibrations obtained in the KNMI-windtunnel usually changed less than 1 percent between half-yearly service checks.

The wind direction signal is a voltage V read from the slider of a potentiometer connected to a supply voltage V_s. During data processing the wind direction δ is computed as a linear function of the voltage V:

$$\delta(\text{deg}) = A(\text{deg}) + B \frac{V}{V_s} \qquad (1)$$

with usually B = 360 deg. The quality of the result is influenced by many error sources, apart from the flow disturbance we will discuss in the next sections:

3.1. The actual plug position may not correspond with the constant A of the calibration formula. The plug azimuth is determined with a sighting tool and a theodolite and is referred to nearby towers. This can be achieved with a 0.1 deg accuracy. It has occured, however, that a plug was turned accidentally.

3.2. The instrument fits rather loosely on the plug, i.e. a notch can be turned 1 or 2 deg before the instrument is fastened with a screw ring. Although a clockwise turn, prior to the fastening , is prescribed, errors cannot be ruled out.

3.3. The position of the potentiometer (i.e. the 0 deg. reading) with respect to the notch on the instrument housing. Although this is usually fixed with a 0.1 deg accuracy, there is a strong suspicion that on rare occasions potentiometers turned during measurements.

3.4. The position of the vane rod with respect to the potentiometer slider. This is fixed during a service check within about 0.1 deg.

3.5. The position of the vane rod compared with the prevailing wind direction depends on the alignment of the vane. In July 1980 a series of 22 Gill 8002 D propeller vanes was tested in the wind tunnel of the National Aerospace Laboratory, NLR. There was a large spread in the position angles of the vanes. The absolute positions with respect to the flow direction were not detected. Compared to the group average the standard deviation was 0.6 deg, with a maximum deviation of 1.2 deg. It is recommended to include this systematic deviation of an individual vane in the calibration constant A.

3.6. Non-linearity of the potentiometer resistance track, either caused by manufacturing inaccuracies or by subsequent detoriation of the resistor surface. Other sources of non-linearity e.g. a bad alignment of potentiometer and vane axes, can be excluded. Potentiometers are tested on linearity and are not accepted if they differ more than 1 deg from the linear calibration. Usually this error remains within a few 0.1 deg.

3.7. The potentiometer-track does not cover the full 360 deg. This "gap" was 3 deg for the vanes and about 6 deg for the propellor instruments. A small gap can also be simulated by the finite contact angle of the potentiometer slider but this factor can be neglected with the present instruments.

The gap was corrected with the old vanes by using an adequate combination of a lower supply voltage than V_s and a higher calibration factor B. The propeller vanes however, have built-in fixed 60 Ω resistors that bridge the missing sectors near 0 deg and 360 deg. Therefore no further correction was necessary.

3.8. The resistance of the wiring between the voltage supply and the terminals of the potentiometer may not be neglected compared to the 5 k Ω potentiometer resistance. The connecting wires could each represent 1-5 Ω. Especially in 1981 this was a serious problem, because the propeller vanes were initially provided with 1 k Ω resistors. Correction for this error was obtained by increasing the supply voltage and subtracting a small angle from A.

3.9. A resistor in series with the slider and also the relatively low input resistance of the signal amplifier (360 kΩ) will cause the reading of V to be lowered with a multiplication factor

$$\{\frac{V}{V_s}(1 - \frac{V}{V_s}) + \frac{p}{5}\}/\{\frac{V}{V_s}(1 - \frac{V}{V_s}) + \frac{p}{5} + \frac{m}{5}\} \qquad (2)$$

for a 5 kΩ potentiometer, where p and m are the series and input resistance respectively (kΩ). A slider resistance of 0.2 kΩ has sometimes been measured, probably due to a bad contact in the plug connector. In such a worst case the maximum error is -0.87 deg for a 5 kΩ potentiometer. This maximum occurs near $V = 0.68\ V_s$. The maximum error is only -0.73 deg without a slider series resistance. For a 1 kΩ-potentiometer it is negligible. Fortunately this error is systematic and a correction is feasible.

Although most of these errors are small they may add up to a quite significant effect. As an example we mention the systematic wind direction errors found during an arbitrarily selected period (September 1979). After the correction for flow disturbance, as described in the next sections, errors of 2 deg or more remained for half of the 16 vanes in the main tower. The maximum errors were 4 resp. 7 deg. This situation can be improved by systematic elimination of the error sources listed above. Also a timely recognition of defective instruments is necessary. This implies routine comparisons of flow-corrected wind data, which can be obtained with the method described in the next sections.

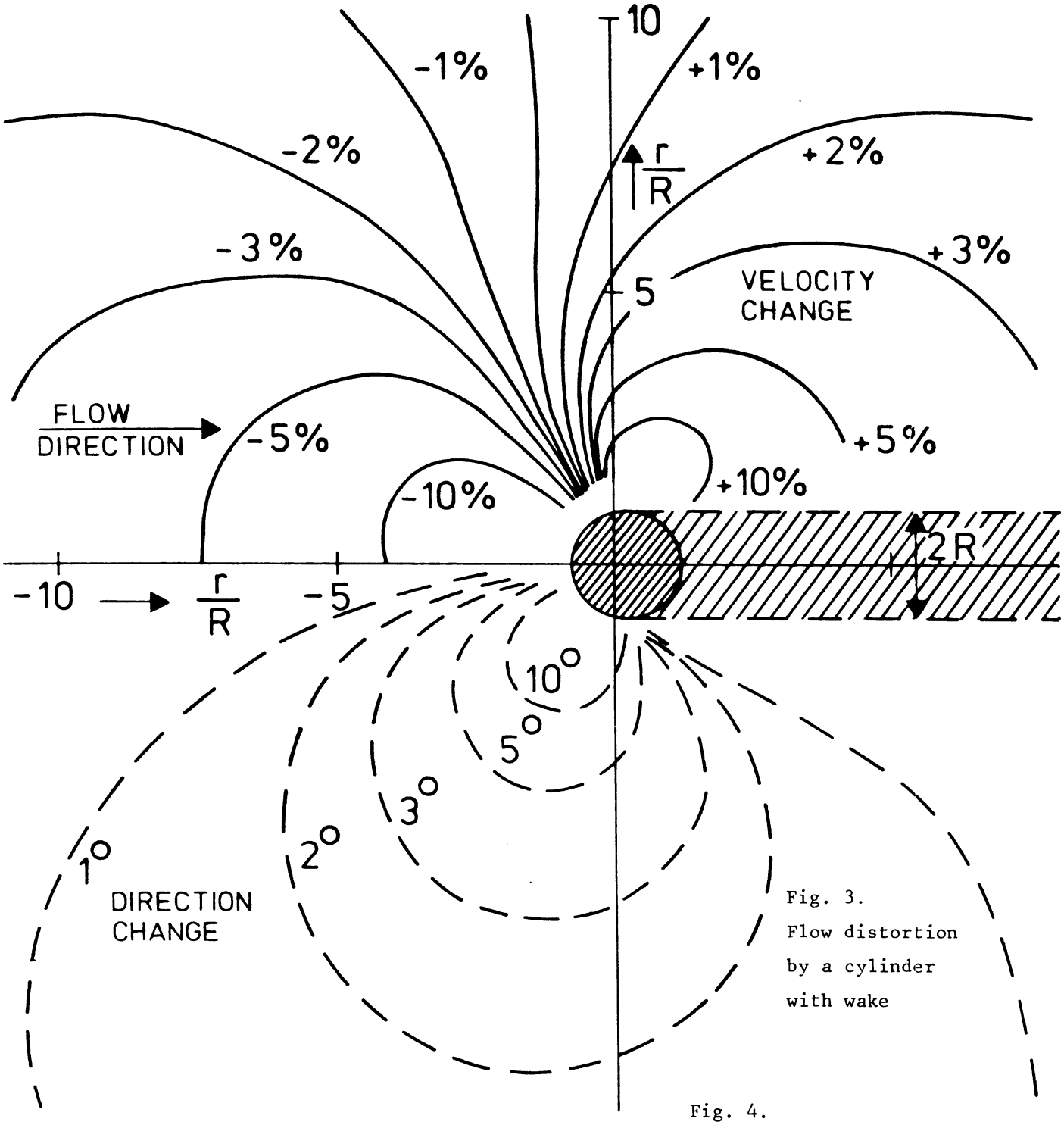

Fig. 3.
Flow distortion by a cylinder with wake

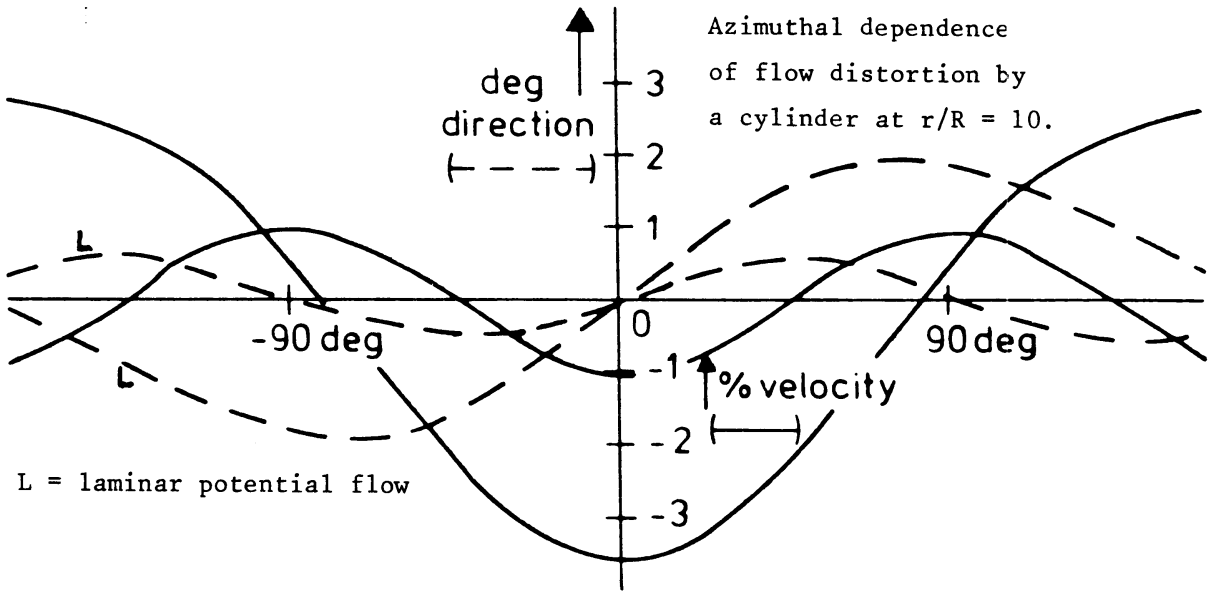

L = laminar potential flow

Fig. 4.
Azimuthal dependence of flow distortion by a cylinder at r/R = 10.

4. Theoretical estimates of the flow disturbance

4. 1. Disturbance of measurements along the main tower

In the following section differences between simultaneous measurements on different booms are compared with simple correction formulae. These expressions are obtained by fitting goniometric functions to the results of potential flow computations. The various contributions to the flow disturbance will be treated separately and finally be added. Most of the potential flow situations we consider are standard problems of potential theory. The theory will be presented in three Appendices. In the following 4 subsections the separate disturbance terms are discussed.

4.1.1. The disturbance by the main tower

The main tower is treated as a vertical cylinder with a wake. The normalized distance of the instrument is r/R = 10. For this problem we can apply the result of Appendix A (Figs. 3 and 4), namely equation A11:

$$\Delta\delta = 2.0 \sin (1.13\ \alpha) \text{ (deg)}$$

$$\frac{\Delta u}{u} = -0.3 - 3.4 \cos (1.19\ \alpha) \text{ (\%)} \qquad \text{(3a.b)}$$

where δ = wind direction and $\alpha = \delta$ - instrument azimuth. The undisturbed wind velocity is u.

These formulae are valid for a restricted range of α only. Furthermore they were derived under the assumption that the drag-coefficient of the tower is independent of the velocity of the flow and of the stability. Moreover we did not account for the presence of balconies. Their influence is small and the observed errors can be explained without considering this aspect (section 5).

4.1.2. The disturbance by the booms

Potential flow parallel to and at an angle with a finite cylinder is treated in Appendices B (Fig. 5) and C (Fig. 6) respectively. To

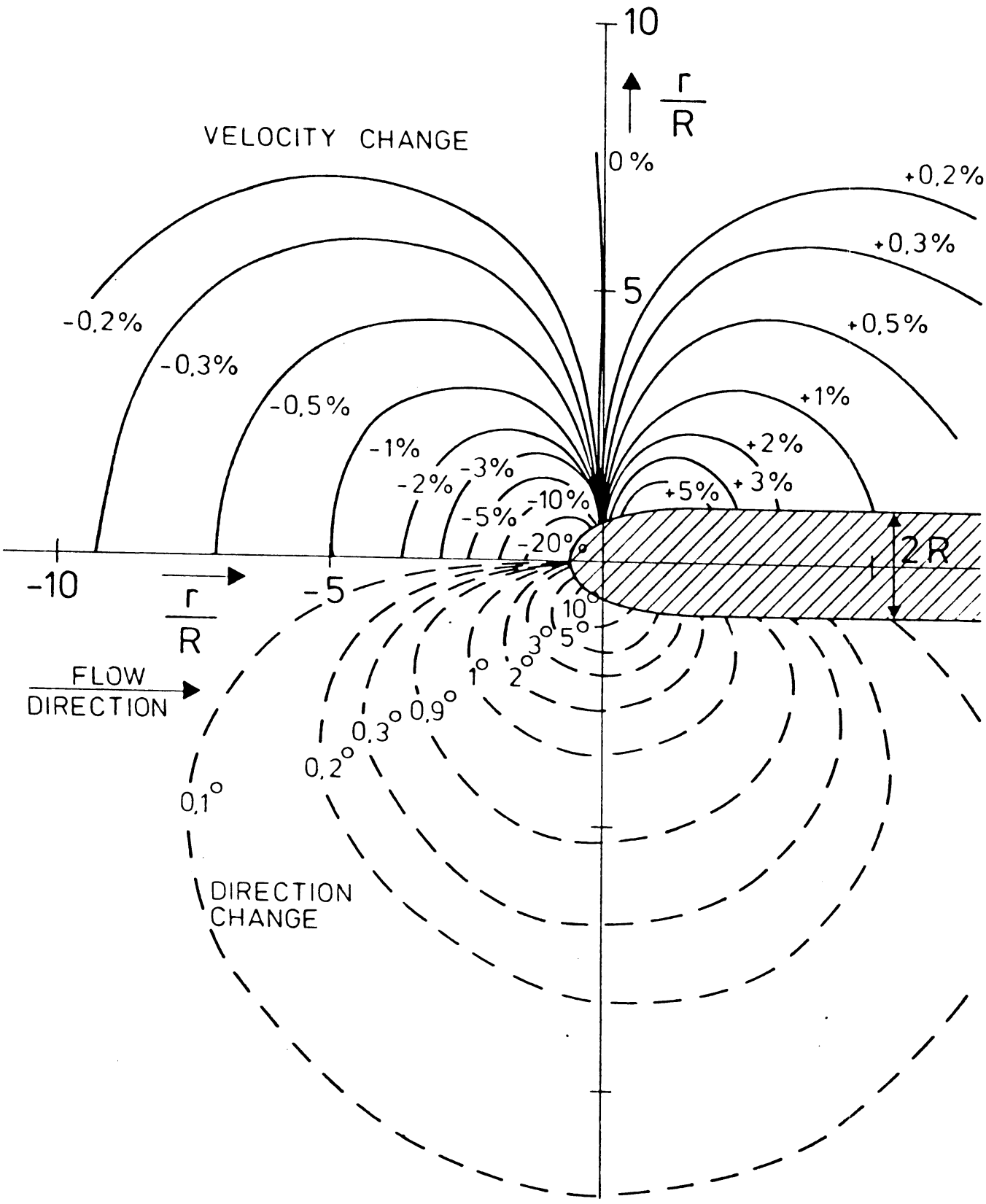

Fig. 5. Flow distortion along a cylinder with rounded top. The error fields are symmetrical around the x-axis.

estimate the boom's influence we have to translate these results for an open-lattice construction.

Although the triangular cross-section of the boom has the same area as an 0.23 m circle, the density of the structure is rather small. This "density" is defined as the ratio between obstructed and free area presented to the flow. Wucknitz (1980) summarizes results from various authors demonstrating that the aequivalent cylinder radius depends on the obstacle dimensions and on the density of the structure. His results show considerable spread but an estimate of R = 0.09 m seems appropriate in the present situation. Then we have from equation C3:

$$\Delta\delta = (-1.20\ ,\ \bar{+}\ 0.60,\ \bar{+}\ 0.40)\ \sin\ (\bar{+}\ \gamma + 45)(\text{deg})$$

$$\frac{\Delta u}{u} = -\ 0.13 + 0.67\ \sin\ (\bar{+}\ \gamma - 20)\quad (\%) \qquad (4a,b)$$

where γ = wind direction - boom azimuth and the $\bar{+}$ signs refer to right and left side arms respectively. The three constants within brackets in Eq. 4a apply in the three measuring periods starting 1973, 1977, 1981 (Table 1: change of plug position).

In the application of this correction even more reservations are necessary than for Eq. 3. Fortunately the present correction is the smaller of the two.

4.1.3. The influence of the side-arms

Here again we may apply the results of the Appendices. The most unfavourable situation existed with the 1973 measurements: an anemometer at a vertical distance of 9 R (R = 0.03 m). For flow perpendicular to a cylinder we find a velocity increase of 0.5% (App. A) and for parallel flow follows a 0.2% increase (App. B). The situation is complicated however, by the finite dimension of the cup system and the asymmetry of its momentum gain, especially in connection with the anemometer's; location near the tip of the side-arm. An anemometer at a left side-arm may therefore run a few 0.1% faster than a right arm instrument. Manifestations of this error will be apparent in the measurements (Fig. 7). However, because of the complexity of this error we will refrain from suggesting a correction. In the years after 1973 the instruments

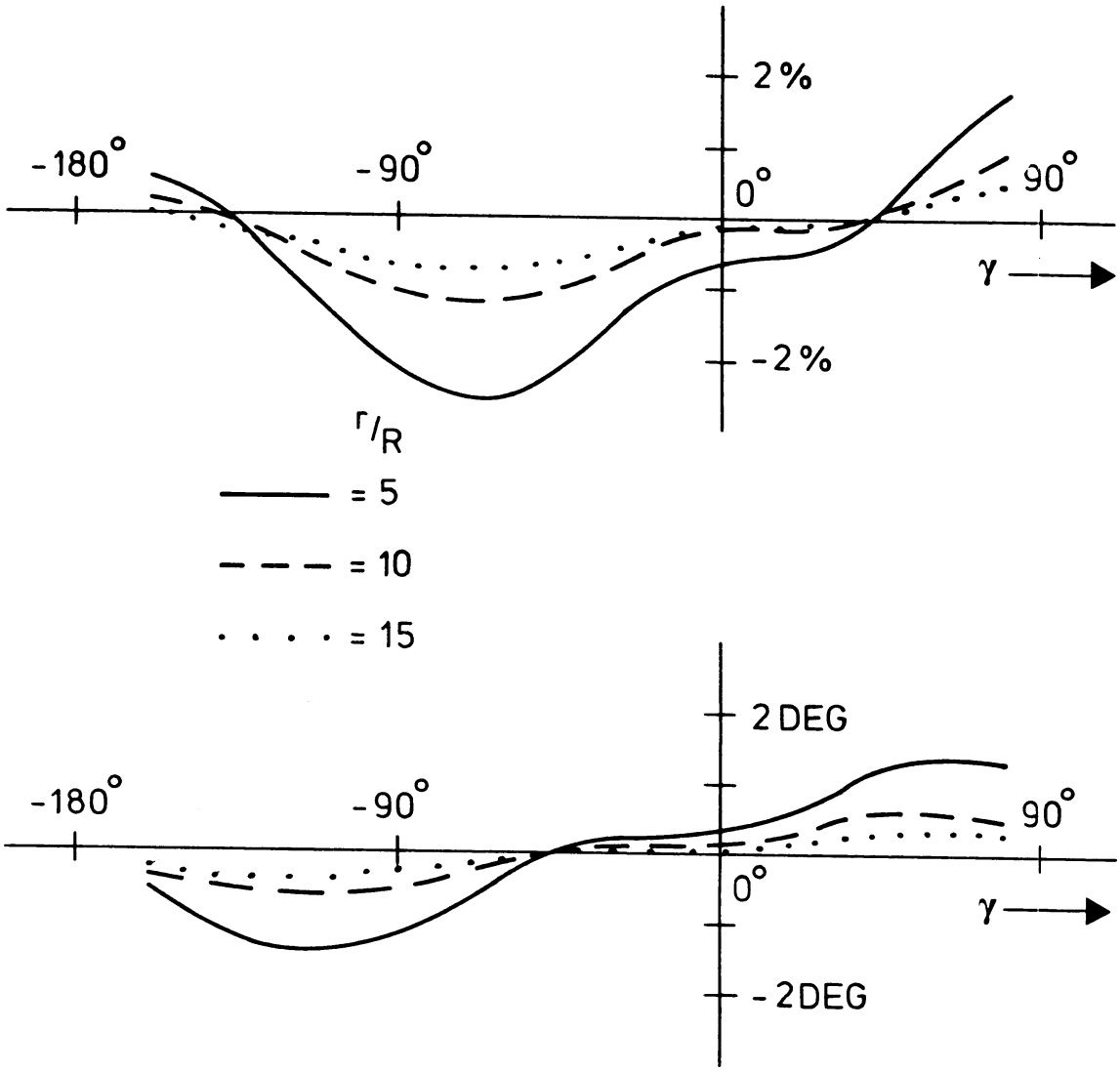

Fig. 6. Numerical approximation of the velocity and direction errors for measurements at a horizontal distance r from the tip of a cylinder with radius R. The flow direction γ is with respect to the boom axis.

were sufficiently high above the side-arms to maintain this error below 0.1 percent.

4.1.4. Contributions by the instrument housing

We may distinguish between errors caused by the instrument itself (e.g. propeller vane) and by another instrument (e.g. a wind vane disturbs a nearby cup system). Due to its symmetry with respect to the flow the velocity disturbance near the propeller vane blades can easily be found from Appendix B. We may replace the housing by an equal-volume sphere of 0.08 m radius. From Fig. 5 we read that a velocity reduction of 0.4% will occur. This error is independent of wind direction and will therefore not show in the comparisons of the next section. The best solution is to calibrate propeller vanes in wind tunnels of sufficiently large cross-section.

In the main mast the influence of the vane on the wind speed measurement might only have been significant during the 1973 measurements. In that year, however, other error sources were more important. The wind speed error due to the vane will certainly have been much less than the 5% (5 min. means) reported from a field experiment by Holub (1970) in the wake of a more massive vane at a shorter distance from the anemometer.

4.2. Measurements on the auxiliary masts

Experimental comparisons for those measurements are hardly feasible because the instruments are too far apart horizontally. Especially at low levels we may attribute a large part of the difference between the measurements to variations in surface roughness. Another problem is the disturbance caused by the measuring building. From inspection of the instrument positions in section 2 we conclude that a combined treatment of the P and T masts and a separate treatment of the M mast must be preferred.

4.2.1. Measurements at the South and North-West masts

These masts are reasonably far from the influence of the main

tower, at least if measurements in its wake are discarded. Also, in constructing these masts, much care has been taken to prevent flow disturbances.

To estimate the disturbance of the 0.07 m diameter vertical supports we may attempt to use the results of Appendix A. At 1 m distance upwind the velocity reduction would be 2%. However, we don't know the effect of the Reynolds number being lower than for the main mast flow. Perhaps more important is the unknown influence of the large size of the instrument compared to the obstacle. In view of these circumstances we will not try to correct this error. The value of 2% is a probable upper bound for this disturbance.

4.2.2. Measurements at the South-East mast (Fig. 2)

The cross-section of this mast has the same area as a 1.0 m radius circle. Following the results of Wucknitz for a construction density 0.3 we may estimate an effective radius of 0.5 m, so that again r/R = 10 at the end of the booms. Therefore eq. 3 also applies to this problem. The influence of the booms can be neglected here because the instruments are nearly above the boom tips at r/R = 8 (See App. B or fig. 5). More serious is the contribution of the main mast: from the results of App. A for a distance of 34 m we conclude that another 30% has to be added to the errors of eq. 3.

Finally we have to mention the flow distortion by the building. If we replace this by a half-sphere of 7.4 m radius we can attempt to use the results of App. B. Fig 5 suggests an upwind reduction of 1.7 per cent. We can check the applicability of Appendix B with a field experiment published by Van der Vliet (1981). He compared two anemometers at 17 resp. 52 m from the tower axis. Unfortunately, these anemometers were at a height of 2 m only and there was no guaranty for the horizontal homogeneity of the terrain. The 17 m anemometer measured 10% lower for upwind flow. According to fig. 5 the difference should have been (11 - 0.6)% if we take the tower axis at $x = \frac{1}{2} R$. This result is encouraging. We may expect this error to change little in the first 10 m above the ground.

As a first approximation we will use this veloicty reduction with the same angular dependence as eq. 3b. A correction for the direction

disturbance by the mast building is not available. From fig. 5 we may expect a few 0.1 deg. From the above considerations we have for the M-mast anemometer (apart from the trivane and anemometer positions in its top which experience about 50% smaller errors):

$$\Delta\delta = 2.6 \sin (1.13\ \alpha) \qquad \text{deg}$$

$$\frac{\Delta u}{u} = -0.7 - 6.5 \cos (1.19\ \alpha) \qquad (\%) \qquad (5a,b)$$

Note that the velocity errors can exceed 7%.

5. Comparison of the estimated errors with experiments

5.1. Velocity measurements

Some experimental values of flow disturbance are available that confirm the results of the Appendices for other towers (e.g. Dabberdt, 1968, Borovenko, 1963, Link, 1960, Wucknitz, 1980, Izumi et al., 1970). Of course we prefer to validate the formulae of section 4 with measurements on the Cabauw tower. Unfortunately no sufficently nearby comparison measurements have been made that could check the low level measurements along the M-mast. The situation along the main tower is more favourable. Two types of simultaneous measurements are available for comparison purposes.

Firstly there were special measurements in 1974 on left and right side arms of the same boom (Van der Vliet, 1981). Secondly we can use the routine measurements on SW1 and Nr after 1977. Some data from earlier years will also be presented to demonstrate qualitatively the disturbance by the side-arms and the connection boxes.

5.1.1. Measurements at the same boom

From Eq. 3b and 4b we can derive the difference in velocity measured at azimuths ±8 deg with respect to the boom direction.

$$(u_r-u_l)/u =$$
$$-3.4\cos(1.19(\gamma-8))+3.4\cos(1.19(\gamma+8))+0.67\sin(-\gamma-20)-0.67\sin(\gamma-20) =$$
$$= -1.12\sin(1.19\gamma)-1.25\sin\gamma \quad (\%) \qquad (6)$$

For small values of γ we may approximate the first term so that we have

$$(u_r-u_l)/u = -2.58\sin\gamma \qquad (6a)$$

The graph can be compared with an experimental result published by Van der Vliet (1981), namely $-2.0\,\gamma$(rad) for measurements obtained in the range $\|\gamma\| < 50$ deg. However, the data concerned which are presented in his fig. 11a would equally well fit with an equation $-2.4\sin\gamma$. Relation 6a is therefore well within the scatter of the measurements.

5.1.2. Measurements on different booms

For short periods in 1978 (anemometers on extension tubes) and 1982 (propellervanes) data have been presented in Figs. 8 and 9. For the differences between the SW1 and Nr positions we have in both years

$$(u_{SW1}-U_{Nr})/u =$$
$$=-3.4\cos(1.19(\delta-242))+3.4\cos(1.19(\delta-378))+0.67\sin(\delta-270)-0.67\sin(-\delta+350)$$
$$= 6.71\sin(1.19(\delta-310)) + 1.02\sin(\delta-310) \quad (\%) \qquad (7)$$

This curve has been plotted in the lower halves of figs. 8 and 9 between the data points concerned. The difference Δu should vanish at $\delta = 310$ deg (and also at $\delta = 130$ deg). At least in 1978 there apparently was a systematic calibration difference between both anemometers. Apart from this we have a good fit in the region where both anemometers are well exposed (310 deg ± 40 deg).

The figures show also clearly the effect of the main mast wake namely near 200 ± 40 deg (N) and 60 ± 40 deg (SW). A minor disturbance is to be seen near $\delta = 20$ deg where the SW1 anemometer comes in the wake of the boom-tip or the side-arm. The same happens near 270 deg with the Nr anemometer. This happens despite the extension tubes. Thanks to the extension tubes, however, the wake-effect is reduced to about 4% compared to 20% in the 1973 situation (fig. 7). It should also be

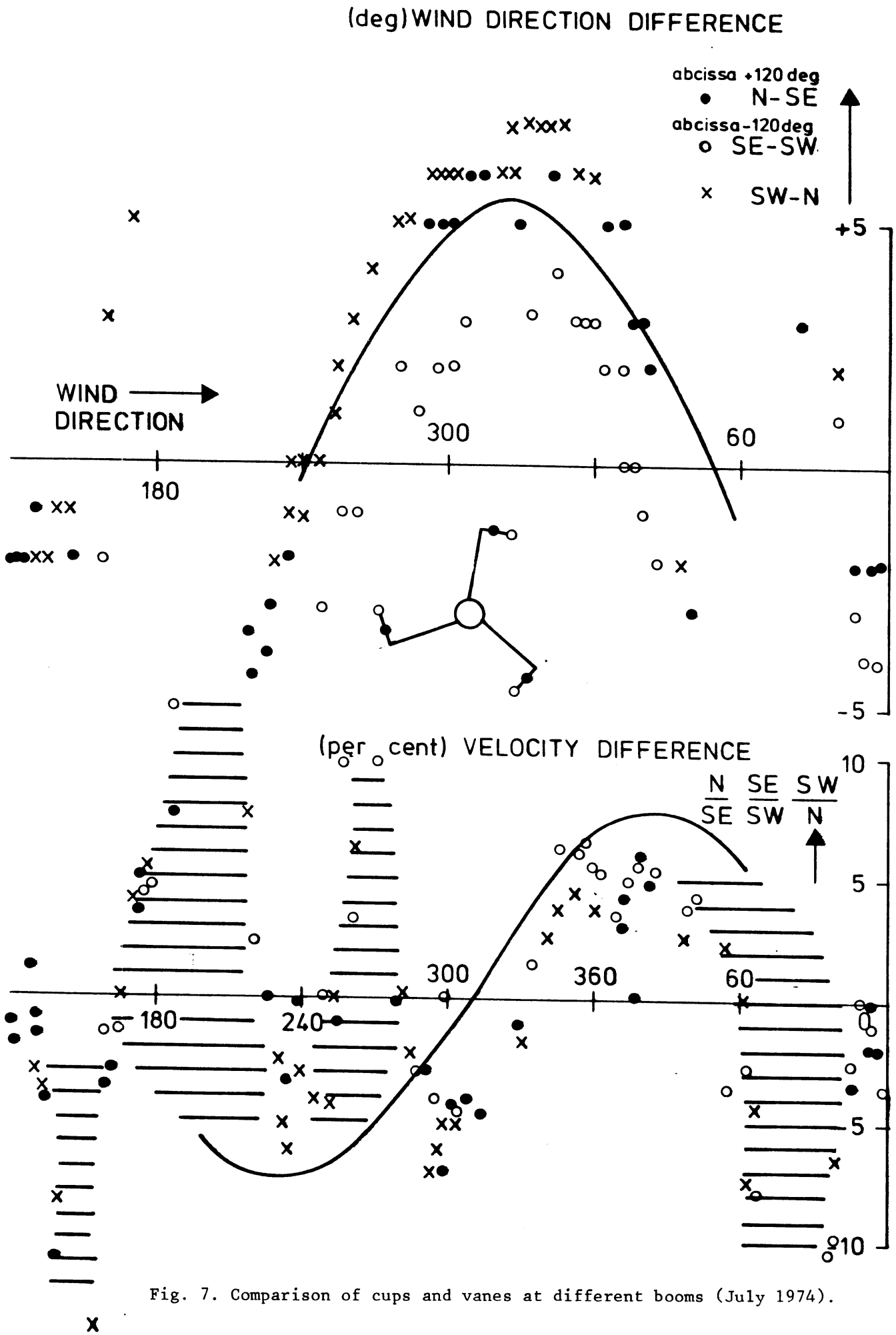

Fig. 7. Comparison of cups and vanes at different booms (July 1974).

stressed that this error is not important because e.g. the N anemometer is selected for $-50 < \delta < 130$ deg only.

The effect of the extension tubes has already been demonstrated in the experiments published by Van der Vliet (1981). His results showed that a length of 0.3 m for the extension tubes was less satisfactory than 0.5 m. Many differences published in the 1981 report, which remained unexplained at that time, can easily be understood with the present flow corrections. Because wind direction errors were not published by Van der Vliet we will also study some of the 1973 data. For reasons of completeness the velocity differences will be included again.

The potential-flow-approximation reads for this situation:

$$(u_{SWr}-u_{Nr})/u = 7.01 \sin(1.15(\delta-318))-1.15 \cos(\delta-290) \qquad (8)$$

This curve has been plotted in the lower half of fig. 7, together with some measured differences. These measurements are only partly explained by the curve. In the absence of extension tubes the wake-effects of the boom tips are quite severe, as was mentioned earlier in this subsection. Differences between theory and experiment occur also at other angles, e.g. around 320 deg. This might be caused by the side arms (see section 4.1.3.). Although fig. 7 shows only differences between two measurements and the actual data are obtained from the least disturbed anemometer, it is still likely that errors up to 2% remain unexplained by the above formula.

The measurements with extension tubes (after 1976) are clearly of much better quality. With the present method flow errors are then predicted within 1% which is usually less than other uncertainties as e.g. calibration errors or the effect of long-term ageing of ball-bearings.

We may conclude that the correction formulae derived in section 4.1. provide a significant improvement for the 1973 data set and that the corrections are even adequate in later years. Figs. 8 and 9 suggest that useful (± 0.5%) velocity measurements are obtained for $-100 < \gamma < 150$ deg at right side arms and $-150 < \gamma < 100$ deg at the left positions. Therefore measurements at two booms (Nr and SW1) are sufficient. With such a configuration 70 deg ranges of overlap are

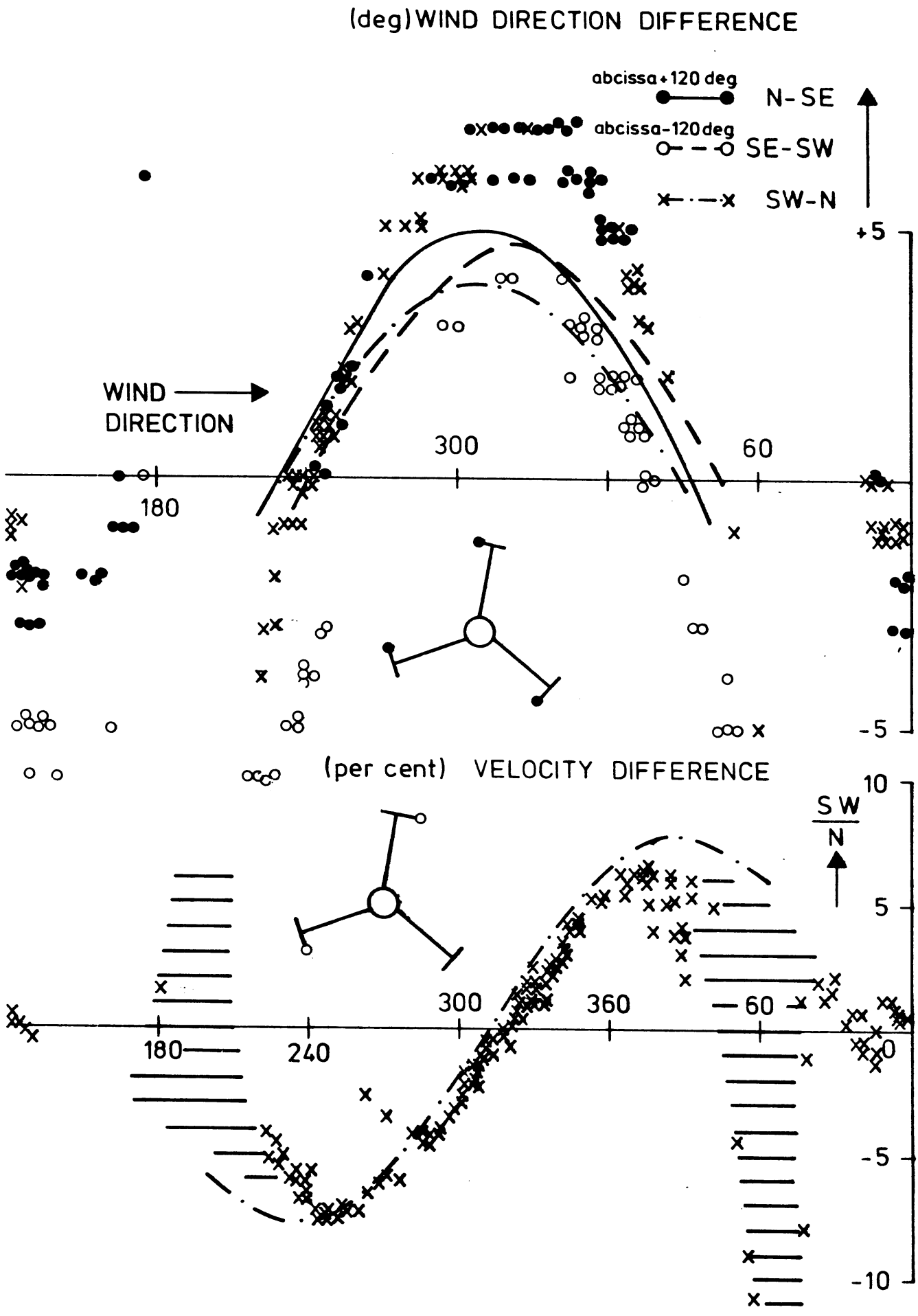

Fig. 8. Comparison of cups and vanes on extension tubes at different booms (Aug., Sep. 1978).

available for routine checks on instrument quality during NW or SE winds.

5.1.3. Possible influence of velocity and stability

Apart from the angular dependence of flow errors also an influence of the Reynolds number or the degree of turbulence can be expected. However, an attempt to stratify the data with regard to wind speed or stability did not offer different results. Of course the scatter of the data points may have obscured these factors.

5.2. Wind direction comparisons

In all the years considered the wind direction was measured on three booms - at least at some of the levels (Table 1). Important changes have been the introduction of extension tubes in 1977 and a new SE construction in 1981. The side-arms were removed and the vanes measured at 1.14 m. above the tip of the boom. Thereby flow errors are reduced to 0.1 deg or less (fig. 5). The new measuring position would also offer an excellent situation for velocity measurements with a propeller vane. It was decided, however, to reserve the SE position for the trivane measurements of special experiments and to quarantee the continuity of the routine measurements by reserving the Nr and SW1 side-arms for that purpose.

5.2.1. Approximation of the wind direction differences

Application of the results of section 4 on the wind measurements specified in section 2 leads for the 1973 measurements to

$$\begin{aligned} \delta_{SWr}-\delta_{Nr} &= 2.0\ \sin(1.13(\delta-252)) - 2.0\ \sin(1.13(\delta-372)) \\ &\quad -1.2\ \sin(-\delta + 295) + 1.2\ \sin(-\delta + 415) = \\ &= 3.70\ \cos(1.13(\delta - 312)) + 2.08\ \cos\ (\delta - 355) \end{aligned} \qquad (9)$$

The differences between the other boom-pairs follow by subtracting 120° from the cosine arguments.

After the change to the mid-plug position on all booms and the

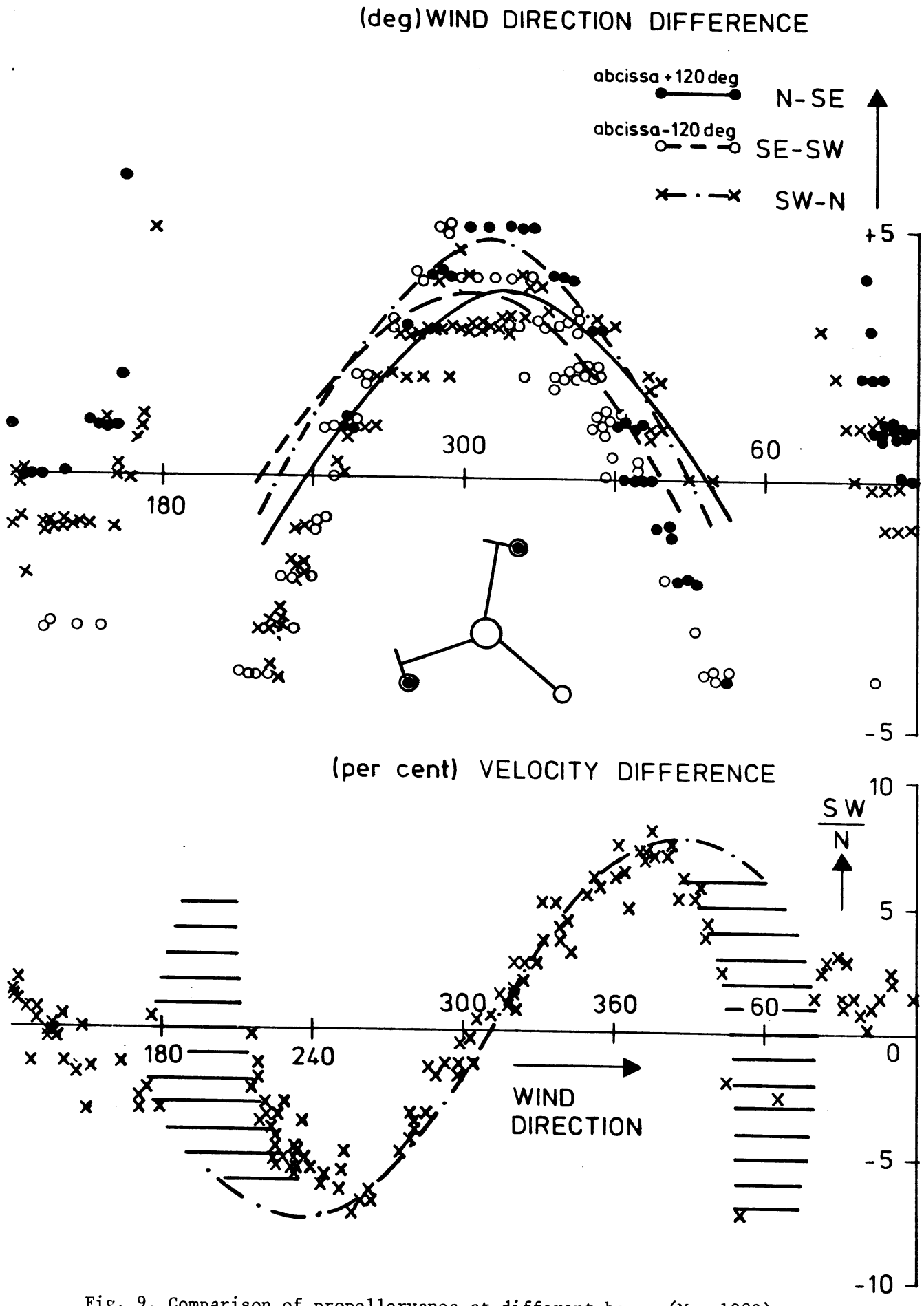

Fig. 9. Comparison of propellervanes at different booms (May 1982).

change to the left side-arm, we have for the measurements between 1977 and 1979

$$\delta_{SWr}-\delta_{Nl} = 3.54 \cos(1.13(\delta-310)) + 0.31 \cos(\delta-310) \quad (10a,b,c)$$
$$\delta_{Nl}-\delta_{SEr} = 3.83 \cos(1.13(\delta-70)) + 1.16 \cos(\delta-70)$$
$$\delta_{SEr}-\delta_{SWr} = 3.70 \cos(1.13(\delta-195)) + 1.04 \cos(\delta-235)$$

For the propeller-vane measurements after 1980 with - on two levels only - an extra wind vane at the SE position:

$$\delta_{SWl}-\delta_{Nr} = 3.89 \cos(1.13(\delta-310)) + 0.77 \cos(\delta-310) \quad (11a,b,c)$$
$$\delta_{Nr}-\delta_{SE} = 3.507 \cos(1.13(\delta-74)) + 0.4 \sin(\delta-55)$$
$$\delta_{SE}-\delta_{SWl} = 3.507 \cos(1.13(\delta-186)) - 0.4 \sin(\delta-205)$$

These seven curves are plotted and compared with measurements in the upper halves of the Figs. 7-9.

5.2.2. Discussion of the wind direction comparisons

As mentioned in section 3 other measuring errors can easily obscure flow disturbances. The scatter in the wind direction measuring points is consequently larger than for the velocity measurements. This large scatter prevented us to attempt a search for non-angular disturbing factors as we tried for the velocity measurements.

Referring to section 3 we can distinguish between errors in B and errors in A of Equation 1. Especially the latter are difficult to separate from flow effects. Errors in B, i.e. an incorrect alignment of the vane's azimuth, must vanish by adding the three mutual wind-direction differences: SW - N + N - SE + SE - SW. Indeed in most of the examples the average value of the measured differences equals the average value of the predictions, at least for wind directions between the booms concerned. An exception is the 1978 case (200 m Aug/Sept) in fig. 8. The average of the measured differences is 5.6 deg while the predcition is 4.4 deg. The only explanation is a non-lineairity in the calibration which implies an angular dependence of B in Eq. 1.

It is worthwhile to recall from section 3 that misalignments of several degrees do occur. The only practical way of tracing these errors is a comparison of winds in sectors between the booms after the measurements have been corrected for flow errors. Then the problem remains that only differences are measured but not the errors of separate vanes. These can only be found by comparisons between higher and lower measuring levels.

Apart from misalignment errors there is also a difference in form of the measured and predicted curves. Especially if the wind direction approaches one of the two boom directions differences of 1 deg or more occur. This behaviour can be explained by the inadequacy of the model for measurements near the wake of the tower (one of the anemometers measures near α = 0 deg but the other near ± 120 deg). Because the selected wind measurements are restricted to $\|\alpha\| < 110$ deg (1982 situation) this deviation of the model does not concern its applicability. This argument holds even stronger for the earlier years with a direction selected between all three vanes so that $\|\alpha\|$ was restricted to about 60 deg.

In the 1978 situation the SE vane was not only necessary to accomplish an unambiguous selection but also to avoid choosing between disturbed N1 and SWr vanes for SE winds. It was a disadvantage, however, that wind speed and direction sometimes then had to be measured at different booms.

5.2.3. An independent field check of the flow errors

The theoretical foundation of the potential flow models in the Appendices involves a rather arbitrary choice of the aequivalent cross-section of a lattice-type construction. Also the measurements are afflicted with a large number of possible errors. Therefore it was decided to make an independent measurement of the vane positions in a few special cases.

The electrical recording of the vane position was eliminated by photographing the SW1 and Nr vanes at the 40 m level from the 60 m balcony with two cameras. The vanes were photographed against a background of two squares laid out on the ground. The sides of the

squares were about 3 m (± 0,005) and the squares were accurately aligned (± 0.1 deg). Averaging of the vane position over at least 5 min. was necessary to eliminate non-simultaneous wind direction fluctuations. Therefore the photographs were taken at nighttime with a 5 or 10 min. exposure. The corners of the squares were marked by small light bulbs switched on briefly during each exposure.

Two photographs for a wind direction near 300 deg were chosen for further analysis. After correction for the perspective caused by the non vertical camera axes we could estimate an angular difference of 4.3 ± 0.5 deg between the vanes, which fits well with the predictions.

6. Conclusions

The theoretical model worked out in the Appendices is confirmed by a variety of instrument comparisons. The flow disturbance errors are rather important: up to 4 per cent in velocity and 3 deg in direction. For the SE-mast the velocity error can reach up to 7 per cent.

Simple wind direction-dependent correction formulae are suggested which enable measurements with propeller vanes to attain an accuracy of better than 1 per cent resp. 1 deg.

From the results an estimate can be given of the useful azimuth range of a certain intrument on a certain position. Also regions of overlap can be defined were flow-corrected measurements on different booms can be compared. These latter comparisons are strongly recommended in order to detect any remaining instrument errors at an early stage.

Due to the flow pattern around the propeller vane-housing it is advised to calibrate these instruments in a wind tunnel with a sufficiently large measuring cross-section.

Although this report applies specifically to the Cabauw measurements, the results described can easily be adapted to study flow disturbance in many other situations.

Appendix A

Potential flow perpendicular to a circular cylinder

The coordinate system in this two-dimensional case is shown in fig. 10. The flow field in this particular situation is obtained by superposition of a disturbance potential $u.\frac{R^2}{r^2}$ on the main flow potential u.x as follows:

$$\phi = u.x(1 + \frac{R^2}{r^2}) \quad , \tag{A1}$$

where R is the radius of the cylinder. The velocity components in an arbitrary point (r,α) follow from

$$u_x = \frac{\partial\phi}{\partial x} = u(1 - \frac{R^2}{r^2} \cos 2\alpha) \tag{A2}$$

$$u_y = \frac{\partial\phi}{\partial y} = u \frac{R^2}{r^2} \sin 2\alpha \tag{A3}$$

In our disturbance study we are interested in the relative error of the velocity vector, i.e.

$$(1 - 2 \frac{R^2}{r^2} \cos 2\alpha + \frac{R^4}{r^4})^{\frac{1}{2}} - 1 \tag{A4}$$

and the angular error in the flow direction

$$\arctan (\frac{\sin 2\alpha}{R^2/r^2 - \cos 2\alpha}) \tag{A5}$$

If we take e.g. r = 10 R we find maximum values of the velocity error -1% at α = 0 or 180 deg and +1% at $\alpha = \pm$ 90 deg. The direction error is largest for α near $\pm$ 45 deg and $\pm$ 135 deg, i.e. 0.6 deg. These errors decline rapidly ($\sim r^{-2}$) with increasing distance from the cylinder.

The flow sketched in fig. 10 disregards the wake that - at these Reynolds numbers of 10^5 or larger - necessarily exists downstream of an obstacle. Such a wake is partly filled with stagnant or even backwards flowing volumes of air. In connection with the main flow the wake may therefore be regarded as a rigid extension of the obstacle. As a consequence the disturbance will depend on r^{-1} instead of r^{-2}. So, even

upstream, the wake may cause important measuring errors.

An analytical treatment of this problem has been presented by J. Wucknitz (1980). The wake is simulated by the potential of a dipole: a source at the origin and a sink of different strength at x = d. Source and sink strength are s_1 and s_2 respectively. The complex potential for this case is written as

$$\phi(z) + i\,\psi(x) = u(z + \frac{s_1}{\pi} \ln z - \frac{s_2}{\pi} \ln(z-d)). \qquad (A6)$$

The velocity potential follows from the real part after replacing z by $r.\exp(i(\pi-\alpha))$ as follows:

$$\phi(z) = u[x + \frac{s_1}{\pi} \ln r - \frac{s_2}{2\pi} \ln\{(r\cos\alpha - d)^2 + r^2 \sin^2\alpha\}], \qquad (A7)$$

and in analogy with Eqs. A2 and A3 we find the velocity components

$$\frac{u_x}{u} = 1 - \frac{1}{\pi}(\frac{s_1}{r}\cos\alpha - s_2 \frac{r\cos\alpha + d}{r^2 + 2dr\cos\alpha + d^2}) \qquad (A8)$$

$$\frac{u_y}{v} = -\frac{1}{\pi}(\frac{s_1}{r}\sin\alpha - s_2 \frac{r\sin\alpha}{r^2 + 2dr\cos\alpha + d^2}) \qquad (A9)$$

Wucknitz chooses $d = R/2$ and presents an example - evidently with the values $s_1 = 4R$ and $s_2 = 3R$. These parameters also determine the wake-cross-section $2R_w$ and the drag coefficient C_D of the cylinder:

$$C_D = \frac{R_w}{R} = \frac{S_1 - S_2}{R} \qquad (A10)$$

The contour of the body simulated in this example is a cylinder centered at $x = \frac{1}{4}$ R connected to a wake with about the same thickness as the cylinder (fig. 2). From Eq. A10 follows a drag coefficient $C_D = 1$. In reality we must take into account the dependence of C_D on the Reynolds number $Re = 2uR/\nu$ (ν is the kinematic viscosity of air) and also on the turbulence of the flow and the surface roughness of the cylinder. For Reynolds numbers between 10^5 and 10^6 C_D may attain a minimum value of about 0.5. This low drag can be expected for wind velocities of a few m. per sec. (R = 1 m). Nakamura et al. (1982) have published experiments for cylinders with very small roughness elements. In their examples a lower drag is reached only for a very restricted range of Reynolds

numbers. Therefore we assume $C_D = 1$ as a first guess.

A two-dimenionsal sketch of the solution of A8 and A9 is shown in fig. 3. Note that, especially because of the wake, considerable errors occur, especially at larger distance from the cylinder. At $\frac{r}{R} = 2$ the errors are almost the same as in the laminar potential flow approximation. At increasing distance the errors no longer decrease with r^{-2} but rather with r^{-1}. An interesting difference in comparison with the flow in absence of the wake is the shift of the azimuth with maximum direction error together with minimum velocity error from near 45 deg to 80 deg or so.

The formulae A8 and A9 become very complicated after conversion to polar coordinates. Therefore we will approximate with simple goniometric formulae as follows:

$$\frac{\Delta u}{u} = \frac{R}{r}\left(-\frac{35R}{r} - 34\cos\left(\left(1 + \frac{1.9R}{r}\right) \cdot \alpha\right)\right) \quad (\%) \qquad \text{(A11a.b)}$$

$$\Delta\delta = \frac{R}{r}\left(1.8 + \frac{20R}{r}\right)\sin\left(\left(1 + \frac{1.3R}{r}\right) \cdot \alpha\right) \quad (\text{deg})$$

where $\Delta\delta$ is the clockwise deviation from the original flow direction. These approximations are sufficiently accurate (0.2% or 0.2 deg) for the range of α used for obtaining data or comparing measurements, i.e. $\|\alpha\| < 120$ deg, at least for $r/R = 10$.

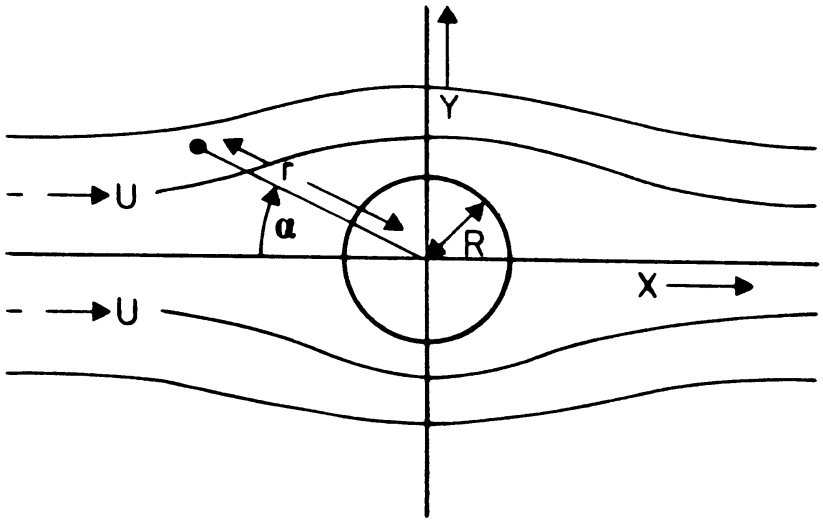

Fig. 10.
Coordinates and streamlines around a circular cylinder.

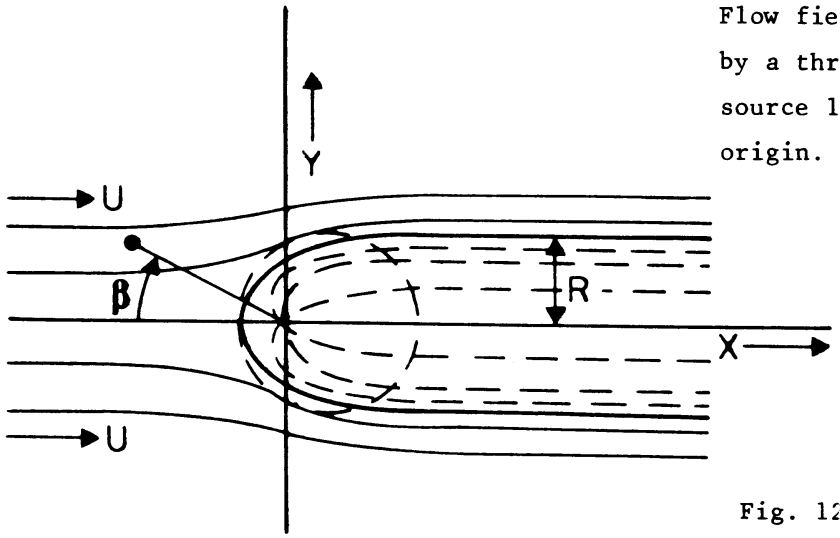

Fig. 11.
Flow field disturbed by a three-dimensional source located in the origin.

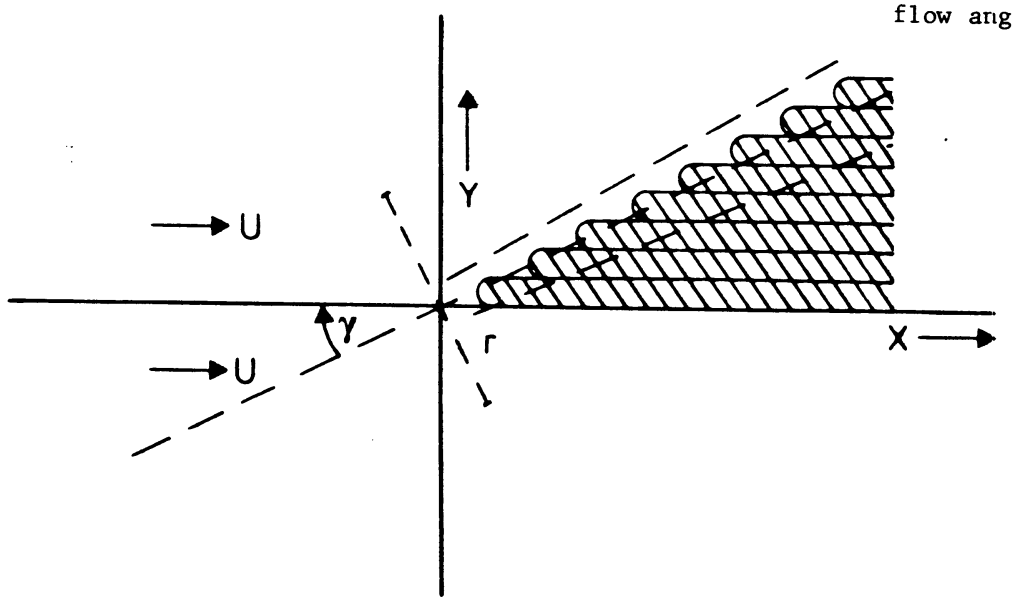

Fig. 12.
Approximation of the boom for varying flow angle γ.

Appendix B

Potential flow parallel to an elongated body

In the first half of the century this flow situation has been studied in connection with airships etc. (e.g. Fuhrman, 1911). The potential flow around a semi-infinite cylinder with rounded top can be approximated by superposing a source in the origin on the undisturbed flow (fig. 11). The resulting potential is

$$\phi = u\,x - u\,\frac{R^2}{4r} \tag{B1}$$

The body so simulated has a contour defined by

$$x = (y^2 - R^2/2)(R^2 - y^2)^{-\frac{1}{2}} \tag{B2}$$

so that the rounded top is located at $x = -R/2$ (see fig. 11).

The velocity field follows from the x and y gradients:

$$\frac{u_x}{u} = 1 - \frac{R^2}{4r^2}\cos\beta \tag{B3}$$

$$\frac{u_y}{u} = \frac{R^2}{4r^2}\sin\beta \tag{B4}$$

We finally have for the relative vector error and the direction error respectively

$$\left(1 - \frac{R^2}{2r^2}\cos\beta + \frac{R^4}{16r^4}\right)^{\frac{1}{2}} - 1 \tag{B5}$$

and

$$\operatorname{acrtan}\left(\frac{\sin\beta}{4r^2/R^2 - \cos\beta}\right) \tag{B6}$$

These equations are illustrated in fig. 5. In contrast to the two-dimensional flow of fig. 2, this error decreases with r^{-2}, so that sometimes a small displacement of an instrument may significantly improve the measurements.

A serious restriction of this treatment is of course its limitation to parallel flow only.

Appendix C

Flow distortion by a semi-infinite cylinder

This is a more general treatment of the situation of Appendix C. In this case, however, no textbook solution is available. Therefore we attempt a superposition of a series of parallel half-cylinders of the type studied in Appendix B. This implies that the wake of the cylinder - no matter which flow angle - plays a significant role.

The flow situation will be described by the angle γ (-180 → 180 deg) between wind direction and boom azimuth and the distance r between the instrument and the boom axis (fig. 12). To simulate an obstacle with average thichness 2R we take cylinders with radius $\frac{2}{\sqrt{\pi}}$ R. Because the side-arms are mounted at some distance in front of the dense part of the booms, we take the first cylinder touching the x-asis and not centered along that axis.

The resulting potential is found from adding a series of potentials of the type B1. The velocity disturbances can then be written for $\gamma \neq 0$:

$$\frac{u_x}{u} = 1 - \frac{R^2}{4r^2} \sum_{n=1}^{\infty} \frac{\cos \arctan\{(\cos\gamma \pm (2n-1)\frac{2}{\sqrt{\pi}})/(\sin\gamma \mp (2n-1)\frac{2}{\sqrt{\pi}} \cot\gamma)\}}{(\sin\gamma \mp (2n-1)\frac{2}{\sqrt{r}} \cot\gamma)^2 + (-\cos\gamma \mp (2n-1)\frac{2}{\sqrt{\pi}})^2} \qquad (C1)$$

$$\frac{u_y}{u} = \frac{R^2}{4r^2} \sum_{n=1}^{\infty} \frac{\sin \arctan\{\cos\gamma \pm (2n-1)\frac{2}{\sqrt{\pi}})/(\sin\gamma \mp (2n-1)\frac{2}{\sqrt{\pi}} \cot\gamma)\}}{(\sin\gamma \mp (2n-1)\frac{2}{\sqrt{\pi}} \cot\gamma)^2 + (-\cos\gamma \mp (2n-1)\frac{2}{\sqrt{\pi}})^2} \qquad (C2)$$

In these formulas the - sign of the ± has to be chosen for $\gamma < 0$. Numerical solutions of C1 and C2 have been used to construct the curves of fig. 6.

A simple check of the method can be obtained for $\gamma = -90$ deg because the velocity reduction component perpendicular to the cylinder should be half the value found for the infinite cylinder of Appendix A. Note also that values for $\gamma = 0$ have to be obtained from Appendix B.

The curves of fig. 6 are intended for evaluating the disturbance by cylindrical booms on measurements with instruments placed on rather thin side-arms. Application to the open construction of the Cabauw booms,

however, is less straightforward. We then have to choose an effective radius for the booms.

In connection with fig. 6 we note that the somewhat irregular behaviour near $\gamma = 0$ can be improved by assuming a less open construction for parallel flow compared to cross flow. Quite probably the wake of the connection boxes then fills a large part of the construction so that the effective radius of the boom increases near $\gamma = 0$.

Taking account of this correction we may attempt a goniometric approximation of the disturbance by open-lattice booms (instruments at left side-arms)

$$\frac{\Delta u}{u} = \frac{R}{r}(-2 + 10 \sin(\gamma-20)) \quad (\%) \qquad (C3a,b)$$

$$\Delta\delta = 6\frac{R}{r}\sin(\gamma + 45) \quad (\text{deg})$$

For instruments at right side arms minus signs have to be inserted for $\Delta\delta$ and γ. These approximations work well in the sector shown in fig. 6. We must keep in mind that measurements outside this range are not relevant because the instruments are then in the wake of the main tower or the boom.

References

G. Fuhrman, 1911/1912. Theoretische und experimentelle Untersuchungen an Ballon Modellen. Jahrbuch der Motorluftschiff - Studiengesellschaft 5, 65-123.

E.V. Borovenko, O.A. Volovoitskii, L.M. Zolotarev, S.A. Isaeva, 1963. Estimation of the effect of the 300-m meteorological mast structure on the wind-gauge readings. pp. 83-92 in: Investigation of the bottom 300-meter layer of the atmosphere. (Ed. N.L. Byzova), Translation Jerusalem 1965.

A. Link, 1966. Uber den Einfluss eines Rohrmastes auf Windgeschwindigkeitsmessungen an demselben. Inst. f. Meteor. Techn. Hochschule Darmstadt.

W.F. Dabberdt, 1968. Tower-induced errors in wind profile measurements. Wind disturbance by a vertical cylinder in the atmospheric surface layer. J. of Appl. Met. 7, 359-366, 367-371.

I. Izumi, M.L. Barad, 1970. Wind speeds as measured by cup and sonic anemometers and influenced by tower structure. J. of Appl. Met. 9, 851-856.

R. Holub, 1970. Wind interference and the placement of anemometers and vanes on open faced towers. Atm. Sci. Group, Univ. of Texas, Coll. of Eng., Rep. 20, Austin, Texas.

A.P. van Ulden, J.G. van der Vliet, J. Wieringa, 1976. Temperature and wind observations at heights from 2 m to 200 m at Cabauw in 1973. KNMI Scientific Rep. 76-7.

J. Wucknitz, 1980. Flow distortion by supporting structures. pp. 605-626 in: Air-Sea Interaction, Instruments and Methods (ed. F. Dobson), New York.

J.G. van der Vliet, 1981. De invloed van de mast en de uithouders op de windmeting te Cabauw. (in Dutch with extended English abstract). KNMI Scientific Rep. 81-4.

Y. Nakamura, Y. Tomonari, 1982. The effects of surface roughness on the flow past circular cylinders at high Reynolds numbers. J. Fluid Mech. 123, 363-378.